Advanced Ceramics Progress: Vol. 12, No. 1, (Winter 2026) 73-80

Materials and Energy Research Center
MERC

Contents lists available at ACERP

Advanced Ceramics Progress

Journal Homepage: www.acerp.ir

Original Research Article

Palmitic Acid Modified Pitch Bonded Doloma Refractories: Correlating Rheology, Microstructure, and Performance

Akbar Davoodi [a] *

[a] *Assistant Professor, Department of Materials Science and Engineering, School of Engineering, Meybod University, 89616-99557, Yazd, Iran.*

* Corresponding Author Email: davoodi@meybod.ac.ir (A. Davoodi)

URL: https://www.acerp.ir/article_258174.html

ARTICLE INFO

Article History:

Received 09 October 2026
Revised 16 November 2026
Accepted 25 November 2026

Keywords:

Pitch Bonded Doloma Refractories,
Palmitic Acid,
Rheological Modification,
Thermal Shock Resistance,
Cold Crushing Strength,
Hydration Resistance

ABSTRACT

Coal tar pitch rheology is a key design parameter that controls the microstructure and performance of pitch-bonded doloma refractories. Palmitic acid was introduced for the first time as a rheological modifier, with an optimum concentration of 6 wt.%. At this level, the modified binder shows simultaneous reductions in softening point, viscosity, and surface tension, while residual carbon decreases only slightly. These improvements promote better particle packing and binder distribution, increasing bulk density from 2.72 to 2.91 g·cm^{-3} and decreasing apparent porosity from 10.8% to 5.9%. Consequently, cold crushing strength increases by approximately 30%. Scanning electron microscopy (SEM) micrographs reveal a refined microstructure with finer pores and enhanced interparticle bonding, yielding a 33% improvement in thermal shock resistance (modulus of rupture, MOR ratio). The 6 wt.% sample also shows a 43% reduction in moisture uptake after 10 days at 25 °C and 95% relative humidity (RH), confirming superior hydration resistance. These findings link binder rheology, microstructure, and performance, showing that engineering the rheology of a carbonaceous binder offers a new design path for optimizing basic refractories without changing the manufacturing route.

https://doi.org/10.30501/acp.2026.606624.1211

1. INTRODUCTION

Doloma-based refractories are among the most important basic refractory materials used in high-temperature metallurgical processes owing to their reasonable price, high refractoriness, excellent compatibility with basic slags, and outstanding resistance to slag corrosion (Ghasemi-Kahrizsangi et al., 2017; Mohammadihooyeh et al., 2020). These refractories are extensively employed in steelmaking (Cai et al., 2021; Mohammadihooyeh et al., 2019; Nag et al., 2020). Their strong affinity for acidic impurities also contributes to efficient desulfurization and dephosphorization during steel refining, making doloma refractories indispensable for the production of clean steels (Shahraki et al., 2024; Zou et al., 2024). Among the various bonding systems, pitch-bonded doloma refractories continue to occupy an important position (Rabah & Ewais, 2009). During tempering, coal tar pitch carbonizes to form a continuous carbonaceous network that binds adjacent refractory particles, providing mechanical integrity and improving resistance to slag penetration and thermal shock. The

Please cite this article as: Davoodi, A. (2026). Palmitic Acid Modified Pitch Bonded Doloma Refractories: Correlating Rheology, Microstructure, and Performance. *Advanced Ceramics Progress*, *12*(1), 73-80. https://doi.org/10.30501/acp.2026.606624.1211

2423-7485/© 2026 The Author(s). Published by MERC.
This is an open access article under the CC BY license (https://creativecommons.org/licenses/by/4.0/).

quality of this network depends critically on the ability of the molten pitch to wet and uniformly penetrate the interparticle spaces during processing (Rocha et al., 2010). Previous studies on doloma refractories have focused predominantly on modifying the refractory aggregate through compositional changes, ceramic additives, nanoparticles, carbon nanomaterials, or surface treatments to enhance density, hydration resistance, and mechanical performance (Díaz-Tato et al., 2022; Gao et al., 2026; Li et al., 2025; Luo et al., 2026; Meng, Wu, Wang, et al., 2026; Meng, Wu, Zheng, et al., 2026; Shahraki et al., 2026; Yi et al., 2023; Zhang et al., 2026a, 2026b). Although these approaches have achieved varying degrees of success, they often require additional raw materials, more complex processing routes, or increased production costs. In contrast, comparatively little attention has been paid to the rheological behavior of the carbonaceous binder itself, despite its fundamental role in governing the evolution of the refractory microstructure and the resulting refractory performance. A systematic understanding of how binder rheology controls the formation of the carbon bonding network, and, ultimately, the multiple performance characteristics of the refractory, therefore remains largely absent.

Limited research has been reported on the use of certain organic acids to improve hydration resistance in basic refractories. However, the specific interaction of palmitic acid with coal tar pitch and its subsequent influence on the processing and performance of pitch-bonded doloma refractories remain entirely unexplored. Unlike previous studies that focused on erucic acid for anode applications, surface-modified magnesia–calcia clinkers, or nanoparticle-reinforced systems (Chen et al., 2004; Wang et al., 2017; Wang et al., 2026), the present work addresses a fundamentally different material system and processing route. The unique physicochemical nature of coal tar pitch, a complex mixture of polycyclic aromatic hydrocarbons with strong intermolecular associations, means that not every fatty acid, oil, or surfactant can serve as an effective rheological modifier. Many organic additives, including common lubricants, paraffins, and surfactants, fail to improve the wetting of doloma aggregates or achieve uniform pitch distribution due to unfavorable interactions with the pitch matrix, often leading to agglomeration and clumping rather than homogeneous dispersion. Simply raising the processing temperature cannot resolve this issue either, as excessive heating causes the pitch to exude from the pores, resulting in island-like segregation and rendering the pressing operation impractical. Thus, the selection of palmitic acid is not arbitrary but stems from its specific molecular structure and interaction mechanism with coal tar pitch, which enables effective rheological modification without compromising binder integrity. This work therefore establishes, for the first time, a direct link between palmitic-acid-modified pitch rheology and the densification, mechanical integrity, thermal shock resistance, and hydration resistance of doloma refractories.

2. MATERIALS AND METHODS

2.1. Raw materials

Natural dolomite ore obtained from the Zefreh mine (Isfahan Province, Iran) was used as the primary raw material. After crushing and particle size classification, the dolomite was calcined and subsequently sintered (at 1750 °C for 32 h) in a rotary kiln to produce sintered doloma, which served as the refractory aggregate for brick fabrication. It should be emphasized that the calcination and sintering processes were conducted sequentially in a single heating stage. The chemical composition of the sintered doloma, determined by X-ray fluorescence (XRF), is presented in Table 1. Coal tar pitch (CTP), supplied by Coal Tar Refining Company (Public Held Co., Isfahan, Iran), was used as the carbonaceous binder. The main physicochemical properties of the pitch, including softening point, viscosity, surface tension, and residual carbon content, are summarized in Table 2. Palmitic acid (hexadecanoic acid, $C_{16}H_{32}O_2$) with a purity of 95 wt.% was incorporated into the molten coal tar pitch as a rheological modifier. Palmitic acid was added at concentrations of 1.5–7.5 wt.%, calculated relative to the weight of the pitch, while unmodified pitch (0 wt.%) was used as the reference. The modified pitch was subsequently used to prepare pitch-bonded doloma refractory bricks.

TABLE 1. Chemical composition of the sintered Zefreh doloma determined by XRF

Oxide	CaO	MgO	Fe_2O_3	SiO_2	Al_2O_3	Na_2O	K_2O
wt.%	57.86	39.89	0.98	0.84	0.23	0.13	0.06

TABLE 2. Physicochemical properties of the coal tar pitch used in this study

Property	Unit	Value
Density	g/cm^3	1.38
Softening point	°C	79
QI*	%	9.8
TI**	%	29.4
Ash content	%	0.35
Residual carbon content	%	52.65
Viscosity (at 170 °C)	mPa.s	3340
Surface tension (at 170 °C)	mN/m	49

* Quinoline Insolubles (indicating solid carbonaceous particles)

** Toluene Insolubles (indicating high molecular-weight resins/β-resins)

2.2. Sample preparation

Prior to brick fabrication, palmitic acid (1.5–7.5 wt.%, relative to the weight of the coal tar pitch) was incorporated into the molten coal tar pitch and thoroughly mixed to obtain a homogeneous modified binder. The sintered doloma aggregates, prepared according to the particle size distribution listed in Table 3, were first introduced into a preheated mixer maintained at 170 °C. The grain size distribution of the sintered doloma was selected based on industrial practices to ensure optimal pressability and maximize the packing density of the green compacts. After approximately 5 min of dry mixing, 7 wt.% coal tar pitch (based on the total weight of the refractory aggregates), either unmodified or modified with palmitic acid, was gradually added to the heated aggregates. Mixing was continued for 10 min to ensure uniform coating of the aggregate particles and homogeneous distribution of the binder throughout the batch. The mixture was then pressed at 160 MPa to produce green bricks. Finally, the specimens were tempered in air at a maximum temperature of 360 °C for 8 h. Except for the palmitic acid content, all processing parameters, including particle size distribution, pitch content, mixing conditions, pressing pressure, and tempering schedule, were kept constant for all specimens.

TABLE 3. Particle size distribution of dead-burned doloma and compositions of the investigated specimens

Sample		P0	P1	P2	P3	P4	P5
Palmitic acid (wt. %)		0	1.5	3	4.5	6	7.5
Doloma particle size distribution (wt. %)	≤ 0.2 mm	3					
	0.2-1 mm	41					
	1-3 mm	36					
	3-5 mm	16					
	5-8 mm	4					
Coal tar pitch (wt. %)		7					

2.3. Characterization

The chemical composition of the samples was determined by X-ray fluorescence spectroscopy (XRF, Bruker S4 Explorer). The microstructure and fracture morphology of the refractory specimens collected from the interior regions of the bricks after service were examined using scanning electron microscopy (SEM, LEO 435VP). The physicochemical properties of the coal tar pitch were determined according to ASTM D3104, ASTM D4715, and ASTM D1331, and using a Bohlin digital rheometer, respectively (Rocha et al., 2005, 2010). The surface tension of the molten coal tar pitch was measured using a tensiometer equipped with a platinum plate. The pitch sample was heated to 170 °C in a temperature-controlled chamber to maintain its molten state. Prior to each measurement, the platinum plate was thoroughly cleaned and flamed to ensure complete wetting. The plate was then brought into contact with the molten pitch, and the surface tension was recorded once a stable equilibrium force was established. The cold crushing strength (CCS) was measured in accordance with ASTM C133. For each composition, five independent specimens were tested (Díaz-Tato et al., 2022). Bulk density and apparent porosity were determined by the kerosene immersion method following ASTM C20. Thermal shock resistance was examined by an oil-quenching method consisting of three thermal shock cycles between room temperature and 1100 °C. In each cycle, the specimens (25 × 25 × 140 mm³) were heated at 1100 °C for 30 min in air and then quenched in oil. After cooling to room temperature, the samples were subjected to the next cycle. Each experiment was repeated with three identical samples, and the results were averaged. Thermal shock resistance was expressed as the ratio of the modulus of rupture after the thermal shock cycles to that before the cycles (Gao et al., 2026; Zhang et al., 2026b). The hydration resistance was evaluated by monitoring the weight gain of the specimens during exposure in a controlled-humidity chamber maintained at 25 °C and 95% relative humidity.

3. Results and discussion

3.1. Rheological properties of coal tar pitch

Figure 1 illustrates the influence of palmitic acid addition on the softening point and residual carbon content of coal tar pitch. Increasing the palmitic acid content from 0 to 7.5 wt.% produced a gradual reduction in the softening point from 79 to 71 °C, indicating a progressive improvement in the thermoplastic behavior of the binder, although the decreasing trend became less pronounced at higher additive contents. In contrast, the residual carbon content was only marginally affected, decreasing from 52.65 wt.% for the unmodified pitch to 49.83 wt.% at 7.5 wt.% palmitic acid, corresponding to a reduction of approximately 3 percentage points. Considering the substantial improvement in rheological characteristics, this slight decrease is unlikely to adversely affect the formation of the carbonaceous bonding phase after coking. This behavior suggests that the modification is dominated by physical interactions rather than chemical degradation of the pitch structure, a hypothesis further supported by the viscosity and surface tension data presented below.

To elucidate the mechanism underlying these rheological modifications, the interaction between palmitic acid (PA) and coal tar pitch (CTP) can be conceptually divided into three sequential stages. In Stage I (surface wetting), the polar carboxyl head group of PA promotes wetting of the pitch surface, consistent with previous observations for erucic acid-modified pitches. In Stage II (molecular intercalation), the long aliphatic chain inserts between the polyaromatic molecules, weakening van der Waals interactions and disrupting the associative network. In Stage III

(molecular loosening), the aromatic molecules become more mobile, reducing resistance to molecular sliding and lowering both the softening point and viscosity (Wang et al., 2017).

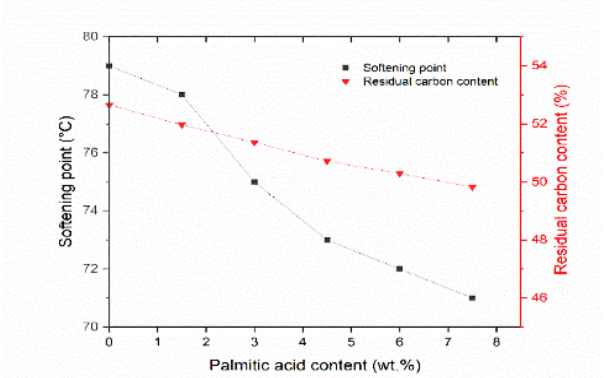


Figure 1. Effect of palmitic acid content on the softening point and residual carbon content of coal tar pitch

Figure 2 presents the corresponding variations in viscosity and surface tension. Both parameters decreased continuously with increasing palmitic acid content. The viscosity decreased from 3340 mPa·s for the unmodified pitch to 410 mPa·s at 7.5 wt.% palmitic acid, representing a reduction of approximately 88%. Similarly, the surface tension decreased steadily from 49 to 29 $mN \cdot m^{-1}$. The simultaneous reduction in viscosity and surface tension is particularly significant in the context of the wetting behavior of the pitch binder during refractory processing. As proposed by Rocha et al., the wetting of aggregate particles by the binder and its subsequent penetration into the interparticle voids are governed by a combination of two independent phenomena: (i) the spreading of the molten binder over the particle surfaces, which is primarily controlled by the liquid–vapor surface tension, and (ii) the flow of the binder throughout the particle network, which is dictated by its viscosity (Rocha et al., 2005; Wang et al., 2017).

The reduction in surface tension (from 49 to 29 $mN \cdot m^{-1}$) substantially promotes more efficient spreading of the modified pitch over the doloma aggregate surfaces. Simultaneously, the 88% reduction in viscosity decreases resistance to viscous flow, allowing the binder to infiltrate narrow capillary channels and fine interparticle voids more readily. The combined effect of these two rheological improvements is a significantly enhanced wetting regime in which the binder can establish more intimate contact with the aggregate surfaces, achieve a more uniform spatial distribution, and fill a larger fraction of the pore space without requiring excessive compaction pressure or elevated processing temperatures. These rheological modifications provide the foundation for the subsequent microstructural evolution, densification behavior, and mechanical performance of the pitch-bonded doloma refractories, which are discussed in detail in the following sections.

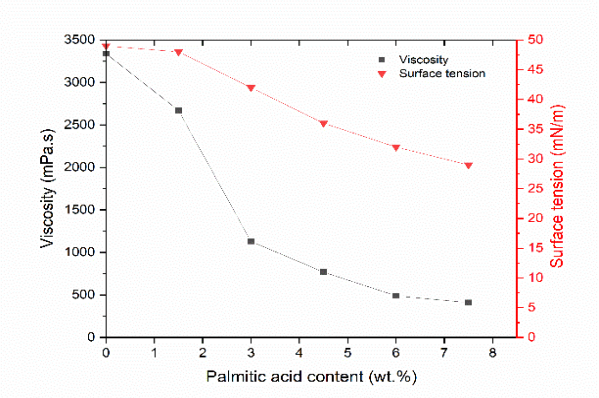


Figure 2. Dependence of viscosity and surface tension of coal tar pitch on palmitic acid content, at 170 °C

3.2. Bulk density and apparent porosity

Figure 3 presents the bulk density and apparent porosity of the pitch-bonded doloma refractories prepared using coal tar pitches modified with different amounts of palmitic acid. An improvement in densification was observed with increasing PA content up to 6 wt.%. The bulk density increased progressively from 2.72 $g \cdot cm^{-3}$ for the reference specimen to a maximum value of 2.91 $g \cdot cm^{-3}$, while the apparent porosity simultaneously decreased from 10.8% to 5.9%. Further increasing the PA content to 7.5 wt.% resulted in a slight decrease in bulk density accompanied by a corresponding increase in apparent porosity, although both parameters remained superior to those of the unmodified specimen. The improved densification can be attributed to the modification of the rheological characteristics of the coal tar pitch. The enhanced wetting promoted particle rearrangement during pressing, increased packing efficiency, and reduced the number of entrapped voids within the green compact. Consequently, tempering produced a more compact carbon-bonded microstructure with fewer and less interconnected pores. The existence of an optimum at 6 wt.% PA indicates that the beneficial effect of increasing binder fluidity is limited. At lower PA contents, the improvement in pitch mobility was insufficient to achieve efficient wetting and complete filling of the interparticle voids. Excessive fluidity may facilitate local binder redistribution during mixing or compaction, resulting in less uniform binder coverage and a slight deterioration in packing homogeneity. The decrease in density at 7.5 wt.% PA may be primarily associated with two factors. First, excessive volatilization of the organic acid during the tempering process could potentially leave behind voids. Second, exceeding the optimal liquid-phase content might disrupt particle packing and increase the distance between adjacent doloma aggregates, potentially hindering the densification process.

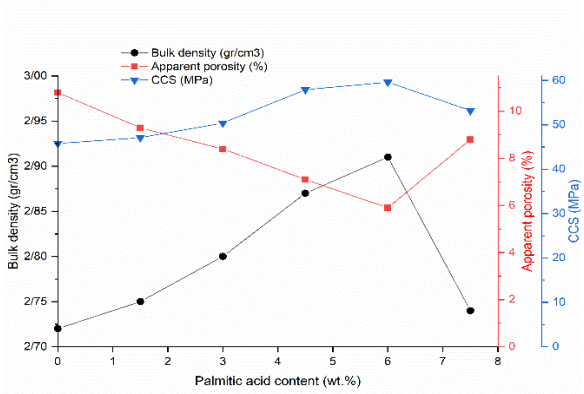


Figure 3. Bulk density, apparent porosity, and cold crushing strength (CCS) of pitch-bonded doloma refractories as a function of palmitic acid content

3.3. Cold crushing strength

Figure 3 also illustrates the CCS of the doloma refractories as a function of PA content. The CCS increased continuously from 45.8 MPa for the reference specimen to a maximum value of 59.6 MPa for P4, corresponding to an improvement of approximately 30%. Further increasing the PA content resulted in a gradual reduction in strength to 53.2 MPa for the specimen containing 7.5 wt.% PA. Nevertheless, all modified specimens exhibited substantially higher compressive strength than the unmodified refractory. The evolution of CCS closely follows the densification behavior, indicating that the mechanical response of the refractories is strongly governed by their microstructural compactness. The increase in bulk density, together with the marked reduction in apparent porosity, decreases both the number and size of critical defects that serve as preferential crack initiation sites during compressive loading. Consequently, the effective load-bearing cross-sectional area increases, and the applied stress is distributed more uniformly throughout the refractory body (Ghasemi-Kahrizsangi et al., 2016; Shahraki et al., 2024). Under compressive loading, stresses are therefore transferred through a larger number of well-connected particle contacts rather than being concentrated around isolated pores or poorly bonded regions. A more homogeneous stress distribution delays crack initiation and reduces the probability of unstable crack propagation, resulting in a significant improvement in compressive strength. The maximum CCS obtained at 6 wt.% PA indicates that this composition provides the optimum balance between binder rheology and microstructural integrity.

3.4. Microstructural characteristics and fracture behavior

Figure 4 shows the fracture morphologies of specimens P0 and P4. SEM observations provide direct microstructural evidence of the structural modifications induced by the rheological optimization of the coal tar pitch. The fracture surface of specimen P0 is characterized by coarse, irregular pores and incomplete bonding between adjacent doloma aggregates. Individual grains remain clearly distinguishable, indicating that only limited interparticle neck formation occurred during tempering. Consequently, the refractory microstructure is discontinuous and contains numerous preferential sites for crack initiation under compressive loading. In contrast, specimen P4 exhibits a considerably more compact fracture surface. Large voids are largely replaced by smaller and more uniformly distributed pores, while adjacent particles are connected through well-developed bonding bridges. The interfaces between neighboring aggregates become less distinct, indicating that the modified pitch produced a more continuous carbonaceous bonding phase capable of establishing stronger cohesion throughout the refractory body. These observations confirm that improving the rheological behavior of the binder enhanced the efficiency of binder distribution during processing and promoted the formation of a more mechanically integrated microstructure after tempering. The fracture morphologies also reveal a noticeable difference in crack propagation behavior. Specimen P0 predominantly exhibits transgranular fracture, in which cracks propagate directly through individual doloma grains, providing a relatively short fracture path and limited resistance to crack propagation. By contrast, crack growth in specimen P4 becomes increasingly intergranular, forcing cracks to deviate repeatedly along particle interfaces. This crack deflection increases the fracture path length and promotes greater energy dissipation before catastrophic failure (Gao et al., 2026; Zhang et al., 2026b). The transition from predominantly transgranular to mixed intergranular fracture therefore provides a microstructural explanation for the higher compressive strength observed in the modified refractories. The SEM observations thus demonstrate that the improvement in mechanical performance originates not solely from reduced porosity but also from the development of a more coherent refractory skeleton, stronger interparticle bonding, and crack propagation paths that are repeatedly deflected along particle interfaces, a toughening mechanism that requires greater fracture energy before catastrophic failure.

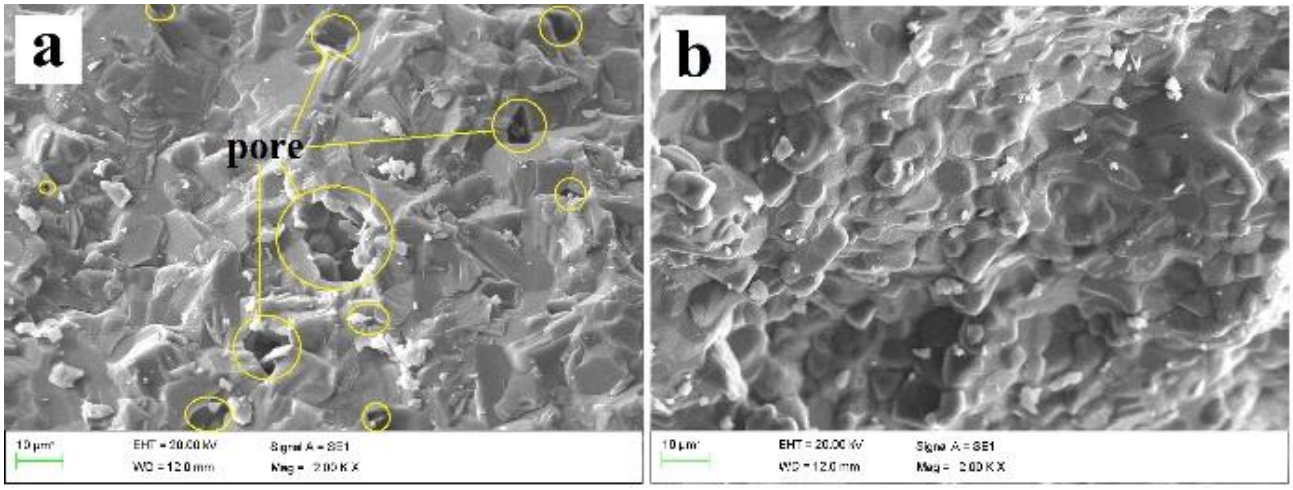


Figure 4. SEM fracture micrographs of pitch-bonded doloma refractories: (a) specimen P0 and (b) specimen P4

3.5. Thermal shock resistance

Figure 5 illustrates the modulus of rupture (MOR) of specimens with different PA contents, both before and after thermal shock exposure. The MOR increased with PA addition up to 6 wt.%, in agreement with the CCS findings, whereas a further increase to 7.5 wt.% led to a decline in MOR. A progressive increase in the MOR ratio was observed, from 38.3% (P0) to a peak value of 71.1% (P4), corresponding to an improvement of approximately 33 percentage points. Beyond this concentration, the MOR ratio decreased to 50.4% at 7.5 wt.% PA (P5).

Thermal shock resistance (R) is described by the equation $R = \sigma_f(1-\nu)/(E\alpha)$. Although reducing porosity increases Young's modulus (E), which inherently has a negative effect on thermal shock resistance, it simultaneously increases fracture strength (σf) significantly. It is important to note that the dependence of strength on porosity is much more pronounced than that of Young's modulus. The increase in strength resulting from reduced porosity appears to have outweighed the increase in Young's modulus, ultimately leading to an increase in the R parameter and improved thermal shock resistance. Furthermore, lower porosity implies fewer stress concentration sites within the microstructure. Pores act as thermal barriers and exacerbate localized thermal stresses by creating inhomogeneities in the temperature distribution. Hence, the specimen with lower porosity not only possesses higher strength but also experiences lower thermal stresses, which together account for its improved thermal shock resistance.

Under thermal cycling, failure depends on both crack initiation and the subsequent propagation of thermally generated cracks. As demonstrated by the microstructural observations, optimization of the binder rheology produced a more coherent refractory body with stronger interparticle bonding and a more tortuous crack propagation path. Such a microstructure suppresses local stress concentrations around structural defects and forces propagating cracks to change direction repeatedly during thermal cycling. The resulting increase in crack path length requires additional fracture energy, thereby delaying catastrophic failure. Similar toughening mechanisms have also been reported for MgO–CaO refractories reinforced with carbon nanofibers and nanotubes (Shahraki et al., 2025; Zhang et al., 2026b).

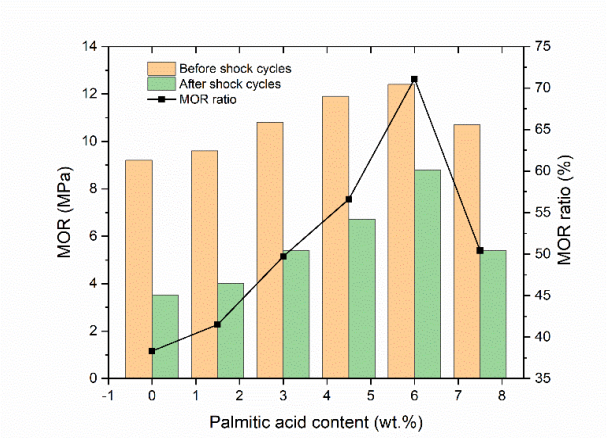


Figure 5. MOR of doloma refractories, before and after thermal shock cycles, and corresponding retained MOR ratio

3.6. Hydration resistance

The hydration resistance of the doloma refractories was evaluated by measuring the weight gain of the specimens during exposure to a controlled humid atmosphere at 25 °C and 95% relative humidity for 10 days (Figure 6). The specimen P0 showed the highest hydration susceptibility, reaching a weight gain of 6.76% after 10 days. Incorporation of PA substantially reduced the hydration rate over the entire exposure period. The lowest weight gain (3.86%) was obtained for the specimen P4, corresponding to a reduction of approximately 43%. Further increasing the PA content resulted in a moderate

increase in weight gain. Formation of calcium hydroxide is accompanied by substantial volumetric expansion, producing internal stresses that progressively damage the surrounding microstructure through crack formation. The resulting increase in pore connectivity facilitates deeper moisture penetration, making the hydration process progressively self-accelerating (Liu et al., 2025; Yeprem, 2007). But in P4, reducion in the continuity of open transport pathways available for water vapor diffusion, led to delaying access of moisture to the reactive CaO phase and slowing the overall hydration process (Dehsheikh et al., 2019). The coincidence of the minimum weight gain with the composition exhibiting the optimum thermal shock resistance and highest density highlights the dominant role of microstructural compactness in controlling hydration resistance (Chen et al., 2007). This approach achieved a significant improvement in hydration resistance without requiring additional processing steps or the incorporation of expensive functional additives, highlighting the practical potential of rheological optimization as a simple and industrially applicable strategy for improving the durability of pitch-bonded doloma refractories (Dehsheikh et al., 2018; Wang et al., 2025).

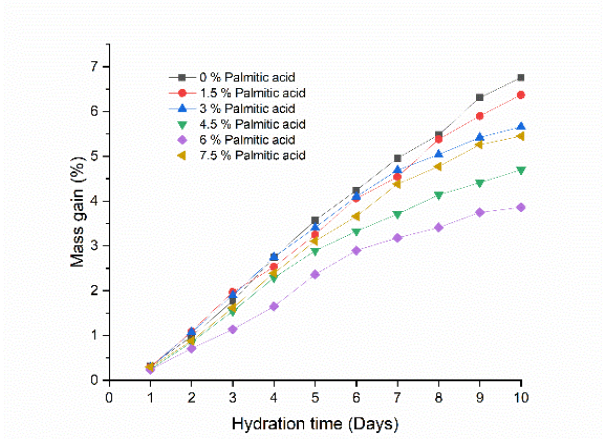


Figure 6. Hydration of doloma refractories containing different amounts of PA at 25 °C and 95% relative humidity

4. CONCLUSIONS

The present study demonstrates that modifying coal tar pitch with palmitic acid is an effective strategy for enhancing the processing characteristics of the binder and the performance of pitch-bonded doloma refractories. The optimum addition of 6 wt.% palmitic acid provides a balance between improved binder rheology and microstructural integrity, yielding the highest densification, mechanical strength, thermal shock resistance, and hydration resistance among the compositions investigated. These improvements originate from a physical plasticization mechanism that preserves the carbon skeleton while promoting more efficient binder distribution and particle packing during processing. It should be clarified that 6 wt.% palmitic acid (PA) was identified as the empirical optimum for this specific system because it exhibited the most consistent and superior overall performance across multiple metrics, including the highest cold crushing strength (CCS), the best thermal shock resistance, and the greatest hydration resistance among all tested specimens. To minimize measurement uncertainty and ensure reliability, CCS was determined in accordance with ASTM C133, with the results averaged over five specimens per composition, while thermal shock resistance was evaluated using the average of three independent specimens. More importantly, the study establishes that binder rheology can serve as an independent design parameter for pitch-bonded doloma refractories, offering an alternative approach to enhancing performance without altering the aggregate composition or the existing manufacturing route.

ACKNOWLEDGEMENTS

The author has no acknowledgements to declare.

REFERENCES

1. Cai, W. K., Liu, J. H., Zhou, C. H., Keeling, J., & Glasmacher, U. A. (2021). Structure, genesis and resources efficiency of dolomite: New insights and remaining enigmas. *Chemical Geology*, *573*, 120191. https://doi.org/10.1016/j.chemgeo.2021.120191

2. Chen, M., Wang, N., Yu, J., & Yamaguchi, A. (2007). Effect of porosity on carbonation and hydration resistance of CaO materials. *Journal of the European Ceramic Society*, *27*(4), 1953–1959. https://doi.org/10.1016/j.jeurceramsoc.2006.05.101

3. Chen, S., Lu, P., Chen, G., & Cheng, J. (2004). Improved hydration resistance of synthesized magnesia–calcia clinker by surface modification. *Journal of the American Ceramic Society*, *87*(12), 2164–2167. https://doi.org/10.1111/j.1151-2916.2004.tb07485.x

4. Dehsheikh, H. G., Ghasemi-Kahrizsangi, S., & Karamian, E. (2018). Addition impact of nano-carbon black on the performance of MgO. CaO compounds. Ceramics International, 44(5), 5524–5527. https://doi.org/10.1016/j.ceramint.2017.12.195

5. Dehsheikh, H. G., Ghasemi-Kahrizsangi, S., Karamian, E., & Shahmohammadian, F. (2019). Hydration resistance improvement of doloma particles using different nanoparticles. Ceramics International, 45(6), 7390–7396. https://doi.org/10.1016/j.ceramint.2019.01.025

6. Díaz-Tato, L., López-Perales, J., Contreras, J. E., Banda-Muñoz, F., Suárez-Suárez, D., González-Carranza, Y., Gómez-Rodríguez, C., & Rodriguez, E. A. (2022). Hydration resistance and mechano-physical properties improvement of a magnesia-dolomite dense refractory by hercynite spinel. *Materials Chemistry and Physics*, *287*, 126314. https://doi.org/10.1016/j.matchemphys.2022.126314

7. Gao, Y., Li, H., Lei, H., Wang, X., Zhang, L., Zhang, H., Huang, Z., & Zhang, S. (2026). Superhydrophobic CNTs/CaCO3-coated MgO-CaO powder for enhancing hydration resistance and high-temperature performance of ultralow-carbon MgO-CaO-C

refractories. *Ceramics International.* https://doi.org/10.1016/j.ceramint.2026.05.239

8. Ghasemi-Kahrizsangi, S., Karamian, E., & Dehsheikh, H. G. (2017). The impact of ZrSiO4 nanoparticles addition on the microstructure and properties of dolomite based refractories. Ceramics International, 43(16), 13932–13937. https://doi.org/10.1016/j.ceramint.2017.07.122

9. Ghasemi-Kahrizsangi, S., Nemati, A., Shahraki, A., & Farooghi, M. (2016). Densification and properties of Fe2O3 nanoparticles added CaO refractories. *Ceramics International*, *42*(10), 12270–12275. https://doi.org/10.1016/j.ceramint.2016.04.173

10. Li, H., Zhang, L., Huang, Z., Zhang, S., & Zhang, H. (2025). Facile preparation of superhydrophobic carbon nanotube coated MgO-CaO grains via densified micro-zone deposition for high-performance MgO-CaO-C refractories. *Journal of the European Ceramic Society*, *45*(16), 117649. https://doi.org/10.1016/j.jeurceramsoc.2025.117649

11. Liu, Z., Cheng, K., Qiu, W., Zhang, R., Pan, S., Gao, Y., Wen, T., Zhang, L., Yuan, L., & Yu, J. (2025). Comprehensive review of the corrosion behavior of magnesia–based refractories by molten steel slag. *Journal of Industrial and Engineering Chemistry*, *145*, 123–143. https://doi.org/10.1016/j.jiec.2024.10.075

12. Luo, J., Li, R., Li, W., Zhou, S., Xu, Z., Liu, B., Chen, C., Bu, N., Mao, X., & Zhang, S. (2026). Superhydrophobicity and In Situ Barrier: A Dual-Functional Coating for Hydration-Resistant MgO-CaO Refractories. *Ceramics International.* https://doi.org/10.1016/j.ceramint.2026.01.006

13. Meng, K., Wu, X., Wang, L., Jiang, J., Zheng, L., Ma, Q., Lin, C., Gao, L., Sun, Z., & Huang, J. (2026). Preparation of self-assembled superhydrophobic coating on MgO–CaO clinker aggregates. *Materials Chemistry and Physics*, *360*, 132614. https://doi.org/10.1016/j.matchemphys.2026.132614

14. Meng, K., Wu, X., Zheng, L., Wang, L., Min, X., Fang, M., & Huang, Z. (2026). Pore-structure Regulation of MgO-CaO Microporous Refractory Aggregates. *Ceramics International.* https://doi.org/10.1016/j.ceramint.2026.01.320

15. Mohammadihooyeh, M., Karamian, E., & Emadi, R. (2019). The impact of MgAl2O4 nano-particles on the hydration-resistance improvement of dolomite-based refractories. *Ceramics International*, *45*(16), 20674–20677. https://doi.org/10.1016/j.ceramint.2019.07.050

16. Mohammadihooyeh, M., Karamian, E., & Emadi, R. (2020). Effect of magnesium-aluminate spinel nano-particles on microstructure and properties behaviors of doloma-containing refractories. *Ceramics International*, *46*(2), 1662–1667. https://doi.org/10.1016/j.ceramint.2019.09.138

17. Nag, M., Nag, B., Agarwal, T., Panigrahi, P., & Singh, B. (2020). Evaluation of suitable refractory for slag dumping area of steel ladle metal zone application for Calcium treated Aluminium killed steel. *Engineering Failure Analysis*, *109*, 104272. https://doi.org/10.1016/j.engfailanal.2019.104272

18. Rabah, M., & Ewais, E. (2009). Multi-impregnating pitch-bonded Egyptian dolomite refractory brick for application in ladle furnaces. *Ceramics International*, *35*(2), 813–819. https://doi.org/10.1016/j.ceramint.2008.02.017

19. Rocha, V. G., Blanco, C., Santamaría, R., Diestre, E., Menéndez, R., & Granda, M. (2005). Pitch/coke wetting behaviour. *Fuel*, *84*(12-13), 1550–1556. https://doi.org/10.1016/j.fuel.2005.02.007

20. Rocha, V. G., Blanco, C., Santamaría, R., Diestre, E., Menéndez, R., & Granda, M. (2010). The effect of the substrate on pitch wetting behaviour. *Fuel Processing Technology*, *91*(11), 1373–1377. https://doi.org/10.1016/j.fuproc.2010.05.007

21. Shahraki, A., Keshavarz, M., Khachatourian, A. M., Nemati, A., & Rezaei, B. (2025). Investigation of hydration, corrosion, and thermal shock resistance of MgO–CaO Ceramic Composites reinforced with electrospun carbon nanofibers. *Materials Research Bulletin*, 113752. https://doi.org/10.1016/j.materresbull.2025.113752

22. Shahraki, A., Khachatourian, A. M., & Nemati, A. (2024). Effect of carbon nanofibers fabricated from electrospun PAN precursors on the characteristics and densification of MgO–CaO ceramic systems. *Journal of the European Ceramic Society*, *44*(14), 116698. https://doi.org/10.1016/j.jeurceramsoc.2024.116698

23. Shahraki, A., Khachatourian, A. M., Nemati, A., & Rezaei, B. (2026). Effect of alumina nanofibers addition on the MgO-CaO compounds characteristics. *Materials Science and Engineering: B*, *324*, 119032. https://doi.org/10.1016/j.mseb.2025.119032

24. Wang, R., Lu, G., Cen, J., & Yu, J. (2017). Effect of erucic acid on the rheological and surface properties of coal tar pitch. International Journal of *Adhesion and Adhesives*, *75*, 108–113. https://doi.org/10.1016/j.ijadhadh.2017.02.014

25. Wang, X., Zhang, L., Li, H., Lei, H., Wang, J., Zhang, H., & Zhang, S. (2026). Low-Cost Facile Fabrication of Superhydrophobic Dual C/CNT–CaCO3 Coated Sintered Doloma Using Waste Oil. *Journal of Environmental Chemical Engineering*, 123099. https://doi.org/10.1016/j.jece.2026.123099

26. Wang, X., Zhang, L., Wang, J., Li, H., Ma, S., Zhang, H., & Zhang, S. (2025). Excellent hydration resistance of CaCO3/CNTs co-modified superhydrophobic doloma grains. *Chemical Engineering Journal*, 168213. https://doi.org/10.1016/j.cej.2025.168213

27. Yeprem, H. A. (2007). Effect of iron oxide addition on the hydration resistance and bulk density of doloma. *Journal of the European Ceramic Society*, *27*(2-3), 1651–1655. https://doi.org/10.1016/j.jeurceramsoc.2006.05.010

28. Yi, N., Ma, Y., Wang, Z., Liu, H., Wang, X., Dong, Y., Xia, Z., Zhu, Y., & Deng, C. (2023). Microstructural regulation and properties enhancement of MgO–CaO ceramics by doping Y2O3. *Journal of Rare Earths*, *41*(11), 1771–1779. https://doi.org/10.1016/j.jre.2022.09.016

29. Zhang, L., Li, H., Wang, X., Gao, Y., Lei, H., Zhang, H., & Zhang, S. (2026a). Construction of superhydrophobic CNT coatings on sintered doloma grains for enhanced hydration resistance. *Powder Technology*, 122574. https://doi.org/10.1016/j.powtec.2026.122574

30. Zhang, L., Li, H., Wang, X., Gao, Y., Lei, H., Zhang, H., & Zhang, S. (2026b). Superhydrophobic CNT-Modified MgO-CaO Grains for Improved Durability and Performance of MgO-CaO-C Refractories. *Journal of the European Ceramic Society*, 118464. https://doi.org/10.1016/j.jeurceramsoc.2026.118464

31. Zou, Y., Chen, D., Cao, J., Xiao, Q., Huang, A., Gu, H., Fu, L., & Yang, S. (2024). The high-efficiency dephosphorization mechanism of steel by a novel porous MgO–CaO based refractories. *Ceramics International*, *50*(18), 34264–34269. https://doi.org/10.1016/j.ceramint.2024.06.245